

Conduction Shape Factor Models for Hollow Cylinders with Nonuniform Gap Spacing

Peter M. Teertstra,* M. Michael Yovanovich,† and J. Richard Culham‡
 University of Waterloo, Waterloo, Ontario N2L 3G1, Canada

DOI: 10.2514/1.35572

An analytical conduction shape factor model is developed for the two-dimensional annular region formed between concentric isothermal cylinders in which the inner and outer boundaries have similar or different shapes. The model is based on the equivalent circular annulus with a modified independent parameter to account for local variations in the gap thickness. Validation of the model is performed using existing numerical data and analytical expressions from the literature for various geometries, including polygonal and rectangular cylinders with a circular hole and the circular cylinder with a polygonal hole. The root-mean-square difference between the data and the model is less than 5% in all cases.

Nomenclature

A	=	cross-sectional area, m ²
A^*	=	dimensionless gap thickness, $\equiv \sqrt{A}/P_i$
A'	=	modified dimensionless gap thickness
d	=	diameter, m
\mathcal{L}	=	general characteristic length, m
N	=	number of polygon sides
n	=	combination parameter
P	=	perimeter, m
r	=	radius, m
s	=	side length, m
S	=	conduction shape factor (per unit length)
$S_{\mathcal{L}}^*$	=	dimensionless shape factor, $\equiv S\mathcal{L}/P_i$
Δ	=	apothem, minimum radial dimension of a polygon, m
δ	=	gap spacing, m

Subscripts

e	=	effective
i	=	inner body
o	=	outer body

Introduction

HEAT conduction within the two-dimensional annular region formed between isothermal nonintersecting inner and outer boundaries is reported in the literature for a variety of geometries. Smith et al. [1] computed the conduction shape factor through electrical resistance measurements for various hollow cylinders, including concentric square cylinders, and square and rectangular cylinders with a centrally located circular hole. Balcerzak and Raynor [2] developed approximate shape factor relationships based on a conformal mapping technique for a large number of geometries: polygonal ($3 \leq N \leq 10$) and rectangular cylinders with a circular hole, eccentric circular cylinders, and the circular cylinder with a

concentric elliptic hole. Lewis [3] extended the conformal mapping method to include additional geometries: the circular cylinder and one-dimensional slab with a polygonal hole. Dugan [4] used a boundary residual technique to predict the conduction shape factor for a square cylinder containing a concentric circular hole. Laura and Susemihl [5] and Laura and Sarmiento [6] also used conformal mapping to simulate the circle in a polygonal cylinder ($3 \leq N \leq 12$) and the polygon ($4 \leq N \leq 8$) in a circular cylinder.

Two analytical models are presented in the literature for the conduction shape factor for the hollow-cylinder problem. Simeza and Yovanovich [7] developed an analytical method based on the parallel flux-tube heat flow model for the polygonal cylinder with a concentric circular hole. The resulting expression for the conduction shape factor (per unit length) is

$$S = 2N \left[\frac{1}{\mathcal{A}\sqrt{\mathcal{A}^2 + \mathcal{B}^2}} \tan^{-1} \left\{ \frac{\sqrt{\mathcal{A}^2 + \mathcal{B}^2}}{\mathcal{A}} \tan \left(\frac{\pi}{N} \right) \right\} \right], \quad (1)$$

$$\mathcal{A}^2 = \ln \left(\frac{\Delta}{r_i} \right), \quad \mathcal{B}^2 = \frac{1}{2}$$

where Δ is the apothem, defined as the minimum radial dimension of the polygon, and r_i is the radius of the inner circle. The model provides an accurate fit of the available data for the hollow triangular, square, and polygonal ($N > 4$) cylinders, and the accuracy of the relationship improves as the size of the inner circular cylinder grows in relation to the outer, such that the local gap spacing becomes more nonuniform.

Hassani and Hollands [8] presented an analytical relationship for the conduction shape factor in annular regions formed between similar boundary shapes, such as the concentric squares, triangles, rhombic cylinders, and rectangles:

$$S = \frac{2\pi}{\ln[1 + (2\pi\delta/P_i)]} \quad (2)$$

where δ is gap spacing and P_i is the perimeter of the inner boundary. This model is applicable only for geometries in which the inner and outer boundaries have similar shapes, such that δ is constant.

There is no analytical model presently available in the literature that predicts the conduction shape factor for the two-dimensional region formed between concentric arbitrarily shaped inner and outer isothermal boundaries.

Model Development

The conduction shape factor for an isothermal three-dimensional convex body was defined by Yovanovich [9] based on the area integral of the dimensionless temperature gradient at the heated surface:

Presented as Paper 4685 at the 38th AIAA Thermophysics Conference, Toronto, Ontario, Canada, 6–9 June 2005; received 8 November 2007; revision received 4 June 2008; accepted for publication 4 June 2008. Copyright © 2008 by the American Institute of Aeronautics and Astronautics, Inc. All rights reserved. Copies of this paper may be made for personal or internal use, on condition that the copier pay the \$10.00 per-copy fee to the Copyright Clearance Center, Inc., 222 Rosewood Drive, Danvers, MA 01923; include the code 0887-8722/09 \$10.00 in correspondence with the CCC.

*Assistant Professor, Department of Mechanical and Mechatronics Engineering, Member AIAA.

†Distinguished Professor Emeritus, Department of Mechanical and Mechatronics Engineering, Fellow AIAA.

‡Professor, Department of Mechanical and Mechatronics Engineering.

$$S = \iint_A -\frac{\partial \phi}{\partial n} dA, \quad \phi = \frac{T(\mathbf{r}) - T_\infty}{T_i - T_\infty} \quad (3)$$

For the two-dimensional annulus, the conduction shape factor per unit depth is calculated based on an integral about the perimeter of the inner heated boundary and can be related to the total thermal resistance between the boundaries, R , by [8]

$$S = \frac{1}{kR} = \frac{Q}{k\Delta T} \quad (4)$$

The shape factor (per unit depth) is nondimensionalized based on an arbitrary scale length \mathcal{L} by the equation

$$S_{\mathcal{L}}^* = \frac{S\mathcal{L}}{P_i} \quad (5)$$

where selecting the perimeter of the inner boundary as the scale length simplifies this relationship between the dimensional and dimensionless conduction shape factors to $S_{P_i}^*$.

Teertstra et al. [10] presented an approximation for the conduction shape factor as a part of a natural convection model for the horizontal annulus. This model was developed based on analysis of the equivalent concentric circular cylinder geometry, for which the exact solution is

$$S_{P_i}^* = \frac{2\pi}{\ln(d_o/d_i)} \quad (6)$$

The inner and outer diameters of this equivalent circular annulus are determined based on a preservation of the inner boundary perimeter P_i and the enclosed cross-sectional area A , as follows:

$$P_i = \pi d_i \rightarrow d_i = \frac{P_i}{\pi} \quad (7)$$

$$A = \frac{\pi}{4}(d_o^2 - d_i^2) \rightarrow d_o = \sqrt{\frac{4}{\pi}A + d_i^2} \quad (8)$$

Substituting these two relationships into Eq. (6) yields the general form of the conduction shape factor model:

$$S_{P_i}^* = \frac{2\pi}{\ln \sqrt{4\pi(A/P_i^2) + 1}} \quad (9)$$

The form of this expression suggests that the independent variables A and P_i can be combined into a single parameter A^* , which represents the dimensionless average gap spacing for the annulus:

$$A^* = \frac{\sqrt{A}}{P_i} \quad (10)$$

The model of Teertstra et al. [10] was validated using natural convection data for a variety of annular geometries, and good agreement between the model and data for low Rayleigh number, conduction-dominated cases was noted when the boundaries had similar shapes or the gap spacing was relatively large. However, when the inner and outer boundaries approach each other, the relative differences between the local gap spacing increase and the heat flow through the shortest path begins to dominate, as shown in Fig. 1 for the square cylinder with a concentric circular hole. Figure 1 also shows the limiting case, in which the diameter of the inner cylinder, d_i , equals the side length of the square cylinder, s_o , and the local gap spacing is reduced to zero. Our physical understanding of the problem predicts that at this limit, the conduction shape factor will become infinitely large due to the thermal short circuit; however, the independent parameter A^* has a finite value at the limit

$$\lim_{\delta \rightarrow 0} A^* = \frac{(d_i^2 - (\pi/4)d_i^2)^{1/2}}{\pi d_i} = \frac{\sqrt{4 - \pi}}{2\pi} \approx 0.1474 \quad (11)$$

Therefore, for the equivalent circular annulus model to correctly predict $S_{P_i}^*$ at the limit $\delta \rightarrow 0$, a modified dimensionless gap spacing

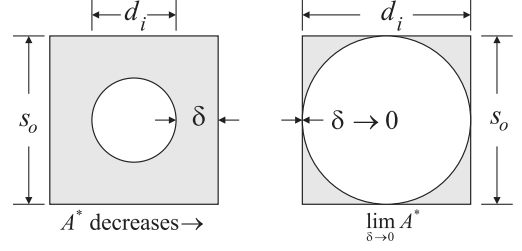


Fig. 1 Square cylinder with a circular hole.

parameter is introduced based on the previously defined independent variable A^* and the limit at zero gap spacing from Eq. (11):

$$A' = [(A^*)^n - (\lim_{\delta \rightarrow 0} A^*)^n]^{1/n} \quad (12)$$

The modified independent parameter A' is then used to calculate the dimensionless conduction shape factor using the general expression

$$S_{P_i}^* = \frac{2\pi}{\ln \sqrt{4\pi(A')^2 + 1}} \quad (13)$$

The effect of reducing the $\delta \rightarrow 0$ limit from the independent variable is that as the gap spacing is reduced and the inner and outer boundaries approach each other, the modified parameter A' approaches zero and the conduction shape factor predicted by Eq. (13) becomes infinitely large. In a manner similar to that used by Churchill and Usagi [11] for the combination of asymptotic solutions, a parameter n has been introduced in Eq. (12) to provide a better fit of the data in the transition region. The integer value $n = 3$ has been selected, which provides good overall agreement based on validation with the available data while retaining the simplicity of the asymptotic method.

Model Validation

Figure 2 shows all the geometries for which numerical data and analytical expressions are available in the literature. The model will be validated for each of the following cases: the polygonal cylinder with a concentric circular hole, the circular cylinder with a polygonal hole, and the rectangular cylinder with a centrally located circular hole. The square cylinder with a circular hole, a special case of the polygonal cylinders from the first row of Fig. 2, will be treated separately due to the large number of studies that have focused on this particular geometry. In each case, the geometry will be described in terms of the dimensions shown in Fig. 2, the limiting value of A^* when $\delta \rightarrow 0$ will be computed, and the model predictions will be compared with the available data. All graphs are plotted using log-log scales that provide straight-line fits for power expressions and emphasize the wide range of values in the results.

Before the validation of annuli with different inner and outer boundary shapes, the accuracy of the equivalent circular annulus model for annuli with similar inner and outer boundary shapes is demonstrated. This comparison includes the data of Smith et al. [1] and Hassani and Hollands [8] for concentric squares, Hassani and

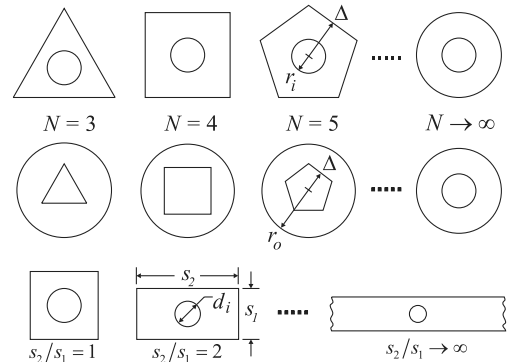


Fig. 2 Schematic of annulus shapes.

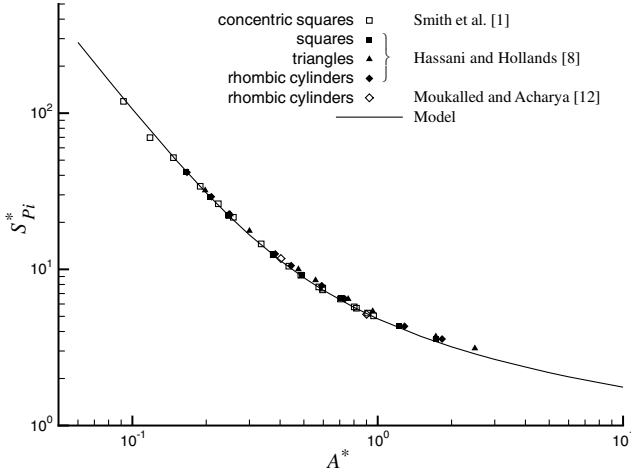


Fig. 3 Model validation for concentric annulus geometries.

Hollands [8] and Moukalled and Acharya [12] for concentric rhombic cylinders, and Hassani and Hollands [8] for concentric triangles. As can be seen in Fig. 3, the model has reduced all the geometries to a single, effective curve for $S_{p_i}^*$ and the agreement between the model and the data is excellent, with an rms difference of 3.4% for all cases.

Square Cylinder with a Circular Hole

In this first case, data from Smith et al. [1], Balcerzak and Raynor [2], Dugan [4], and Laura and Susemihl [5] and the analytical expression of Simeza and Yovanovich [7] are compared with the model for the square cylinder with a concentric circular hole. The dimensionless gap spacing, based on the dimensions shown in Fig. 2, is

$$A^* = \frac{1}{\pi} \sqrt{\left(\frac{s_o}{d_i}\right)^2 - \frac{\pi}{4}} \quad (14)$$

The limiting value of the dimensionless gap spacing is calculated as described in the previous section:

$$\lim_{\delta \rightarrow 0} A^* = \frac{\sqrt{4 - \pi}}{2\pi} \quad (15)$$

Figure 4 compares the model with the data and clearly demonstrates both the asymptotic behavior of the system when the local gap spacing $\delta \rightarrow 0$ as well as the accuracy of the model, with an rms difference of 4.7% for the data and 4.5% for the analytical model of Simeza and Yovanovich [7].

Polygonal Cylinder with a Circular Hole

The numerical data of Laura and Susemihl [5] and Balcerzak and Raynor [6] and the analytical model of Simeza and Yovanovich [7] are compared with the equivalent circular annulus model for three different polygonal cylinders ($N = 3, 5,$ and 10), each containing a centrally located circular hole. The dimensions are defined as shown in Fig. 2 using the inner circle radius r_i and the apothem of the polygon Δ , defined as the minimum radial distance from the center to the edge. Given the following relationship for the area of a polygon,

$$A = N\Delta^2 \tan \frac{\pi}{N} \quad (16)$$

where N equals the number of sides of the polygon, the dimensionless gap spacing evaluates to

$$A^* = \frac{1}{2\pi} \sqrt{N \tan \frac{\pi}{N} \left(\frac{\Delta}{r_i}\right)^2 - \pi} \quad (17)$$

The limiting value of A^* when $r_i = \Delta$ is

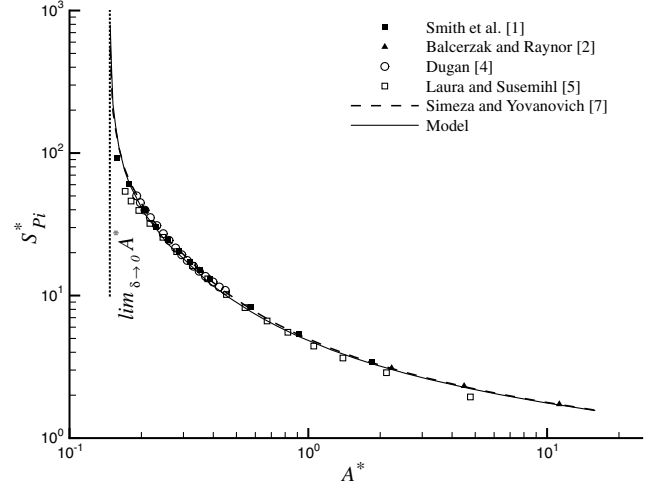


Fig. 4 Model validation for a square cylinder with a concentric circular hole.

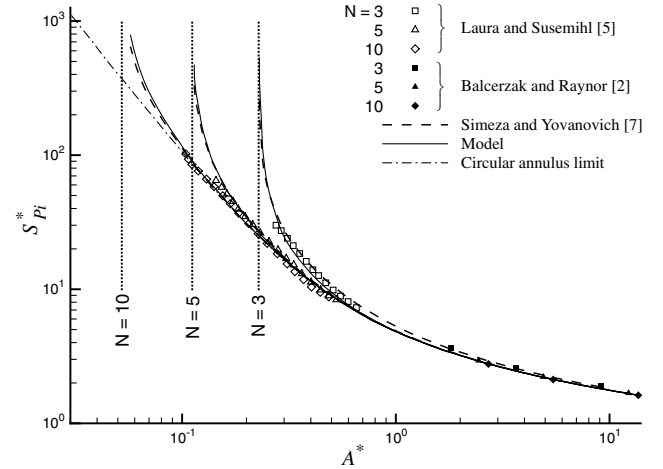


Fig. 5 Model validation for a polygonal cylinder with a concentric circular hole.

$$\lim_{\delta \rightarrow 0} A^* = \frac{1}{2\pi} \sqrt{N \tan \frac{\pi}{N} - \pi} \quad (18)$$

From Fig. 5 it can be shown that the model does a good job of predicting the trends of the solution, providing a good fit to many of the experimental data points and the analytical model of Simeza and Yovanovich [7]. Agreement between the data and the model is best for the $N = 10$ polygon; the rms difference for the $N = 10$ and 5 cases is 3%. In the case of the triangular cylinder, the difference between the data and the model increases to 8.8% due to the significant differences between the local gap thicknesses when $N = 3$ and the approximate nature of a model based on equivalent circles.

Circular Cylinder with a Polygonal Hole

The model is next validated with data of Laura and Sarmiento [6] for the circular cylinder with a concentric polygonal hole, as presented in Fig. 6. Three different geometries are compared with the model predictions: square ($N = 4$), hexagonal ($N = 6$), and octagonal ($N = 8$) polygons. The area of the polygon is determined from Eq. (17), the inner boundary perimeter for the polygon is

$$P_i = 2N\Delta \tan \frac{\pi}{N} \quad (19)$$

and the dimensionless gap spacing evaluates to

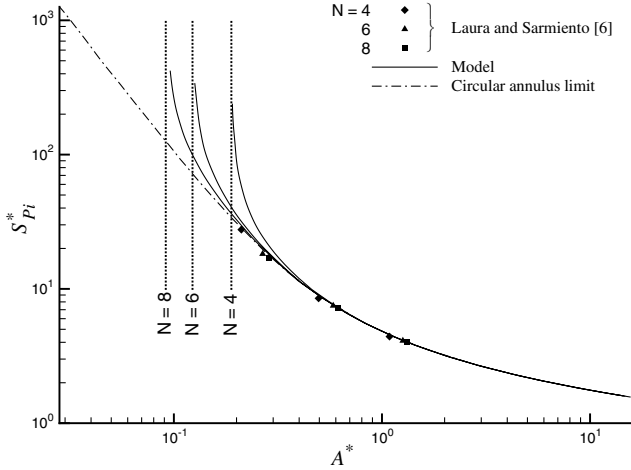


Fig. 6 Model validation for a circular cylinder with a concentric polygonal hole.

$$A^* = \frac{\sqrt{\pi(r_o/\Delta)^2 - N \tan(\pi/N)}}{2N \tan(\pi/N)} \quad (20)$$

At the limit when the vertices of the polygon approach the circular boundary, the dimensionless gap spacing becomes

$$\lim_{\delta \rightarrow 0} A^* = \frac{\sqrt{\pi - (N/2) \sin(2\pi/N)}}{2N \sin(\pi/N)} \quad (21)$$

The data available in the literature are limited to large values of dimensionless gap spacing only, such that when they are plotted in terms of A^* , all the points fall on the same curve and there is no clear distinction between the three different geometries. The rms difference between the model and the data is 5.5% for all cases. Additional data for A^* values near the lower limit would be helpful in completing the validation of the model for this type of annulus.

Rectangular Cylinder with a Circular Hole

The final model validation involves a rectangular cylinder with a cross section of $s_1 \times s_2$ with a centrally located circular hole. Numerical data of Smith et al. [1] and Balcerzak and Raynor [2] are compared with the model predictions for a wide range of aspect ratios, varying from an almost-square cylinder with $s_2/s_1 = 1.2$ to 5, which approaches the behavior of the semi-infinite slab. The dimensionless gap spacing in this case is determined by

$$A^* = \frac{1}{\pi} \sqrt{\frac{s_2}{s_1} \left(\frac{s_1}{d_i}\right)^2 - \frac{\pi}{4}} \quad (22)$$

where, at the limit of $\delta \rightarrow 0$, A^* reduces to

$$\lim_{\delta \rightarrow 0} A^* = \frac{1}{\pi} \sqrt{\frac{s_2}{s_1} - \frac{\pi}{4}} \quad (23)$$

When $s_2/s_1 \leq 1.5$, the model is in good agreement with the data of Smith et al. [1] as shown in Fig. 7, with an rms different of 4% for all values of A^* . However, for $s_2/s_1 \geq 2$, the data of Balcerzak and Raynor [2] indicate that the conduction shape factor is dependent on aspect ratio. Because this functional dependence is not included in the effective circular annulus model, an alternate formulation is proposed based on the analytic solution for the infinite one-dimensional slab with a circular hole at its centerline [9]:

$$S_{Pi}^* = \frac{2\pi}{\ln[(4/\pi)(s_1/d_i)]} \quad (24)$$

where the ratio of the slab thickness s_1 over the cylinder diameter d_i is related to the existing modified independent parameter A' by solving the following equation for s_1/d_i :

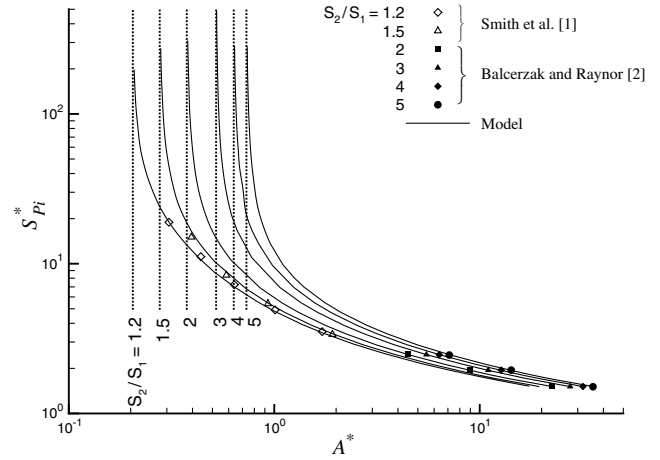


Fig. 7 Model validation for a rectangular cylinder with a concentric circular hole.

$$A^* = \frac{1}{\pi} \sqrt{\frac{s_2}{s_1} \left(\frac{s_1}{d_i}\right)^2 - \frac{\pi}{4}} \quad (25)$$

Substituting the modified independent parameter A' for A^* as in the previous cases yields

$$\frac{s_1}{d_i} = \sqrt{\frac{\pi^2(A')^2 + \pi/4}{s_2/s_1}} \quad (26)$$

Figure 7 compares the data of Balcerzak and Raynor [2] for $s_2/s_1 = 2-5$ with the model from Eqs. (24) and (25) and shows good agreement between the two, with an rms difference of less than 1% for all cases. As in the previous case, additional data for smaller A^* values would be helpful to complete the validation for this geometry.

Conclusions

A model has been developed to predict the dimensionless conduction shape factor in the annular region formed between isothermal inner and outer boundaries having similar or different shapes. Based on the equivalent circular annulus, the method uses a modified independent parameter to account for the thermal short circuit that occurs when the inner and outer boundaries approach each other and the local gap thickness approaches zero. The model has been validated using numerical data from the literature for a variety of geometries, including various combinations of concentric polygonal, rectangular, and circular cylinders. The rms difference between the data and the model was less than 5% in most cases, with the largest difference of 9% rms occurring in the case of the triangular cylinder with a concentric circular hole.

References

- [1] Smith, J. C., Lind, J. E., and Lermond, D. S., "Shape Factors for Conductive Heat Flow," *AIChE Journal*, Vol. 4, No. 3, 1958, pp. 330–331. doi:10.1002/aic.690040319
- [2] Balcerzak, M. J., and Raynor, S., "Steady State Temperature Distribution and Heat Flow in Prismatic Bars with Isothermal Boundary Conditions," *International Journal of Heat and Mass Transfer*, Vol. 3, No. 2, 1961, pp. 113–125. doi:10.1016/0017-9310(61)90074-6
- [3] Lewis, G. K., "Shape Factors in Conduction Heat Flow for Circular Bars and Slabs with Various Internal Geometries," *International Journal of Heat and Mass Transfer*, Vol. 11, No. 6, 1968, pp. 985–992. doi:10.1016/0017-9310(68)90004-5
- [4] Dugan, J. P., "On the Shape Factor for a Hollow, Square Cylinder," *AIChE Journal*, Vol. 18, No. 5, 1972, pp. 1082–1083. doi:10.1002/aic.690180537
- [5] Laura, P. A. A., and Susemihl, E. A., "Determination of Heat Flow Shape Factors for Hollow Regular Polygonal Prisms," *Nuclear Engineering and Design*, Vol. 25, No. 3, 1973, pp. 409–412. doi:10.1016/0029-5493(73)90036-8

- [6] Laura, P. A. A., and Sarmiento, G. S., "Heat Flow Shape Factors for Circular Rods with Regular Polygonal Concentric Inner Bore," *Nuclear Engineering and Design*, Vol. 47, No. 2, 1978, pp. 227–229.
doi:10.1016/0029-5493(78)90064-X
- [7] Simeza, L. M., and Yovanovich, M. M., "Shape Factors for Hollow Prismatic Cylinders Bounded by Isothermal Inner Circles and Outer Rectangular Polygons," *International Journal of Heat and Mass Transfer*, Vol. 30, No. 4, 1987, pp. 812–816.
doi:10.1016/0017-9310(87)90213-4
- [8] Hassani, A. V., Hollands, K. G. T., and Raithby, G. D., "A Close Upper Bound for the Conduction Shape Factor of a Uniform Thickness 2D Layer," *International Journal of Heat and Mass Transfer*, Vol. 36, No. 12, 1993, pp. 3155–3158.
doi:10.1016/0017-9310(93)90044-7
- [9] Yovanovich, M. M., "Conduction and Thermal Contact Resistances (Conductances)," *Handbook of Heat Transfer*, 3rd. ed., edited by J. H. Hartnett, W. M. Rohsenow, and Y. Cho, McGraw–Hill, New York, 1998, pp. 3.1–3.78.
- [10] Teertstra, P., Yovanovich, M. M., and Culham, J. R., "Analytical Modeling of Natural Convection in Horizontal Annuli," 43rd AIAA Aerospace Sciences Meeting and Exhibit Conference, Reno, NV, AIAA Paper 2005-0959, Jan. 2005.
- [11] Churchill, S. W., and Usagi, R., "On the Shape Factor for a Hollow Square Cylinder," *AIChE Journal*, Vol. 18, No. 6, 1972, pp. 1121–1128.
doi:10.1002/aic.690180606
- [12] Moukalled, F., and Acharya, S., "Laminar Natural Convection Heat Transfer in an Eccentric Rhombic Annulus," *Numerical Heat Transfer, Part A, Applications*, Vol. 26, No. 1, 1994, pp. 551–568.
doi:10.1080/10407789408956009